

EFFECT OF CHLORIDE IONS ON THE STRUCTURAL, OPTICAL, MORPHOLOGICAL, AND ELECTROCHEMICAL PROPERTIES OF Cu_2O FILMS ELECTRODEPOSITED ON FLUORINE-DOPED TIN OXIDE SUBSTRATE FROM A DMSO SOLUTION

G. RIVEROS^{1,*}, M. LEÓN^{1,2}, D. RAMÍREZ¹

¹Instituto de Química y Bioquímica, Facultad de Ciencias, Universidad de Valparaíso, Avenida Gran Bretaña, 1111, Playa Ancha, Valparaíso, Chile.

²Departamento de Química, Universidad Técnica Federico Santa María, Avenida España 1680, Valparaíso, Chile.

ABSTRACT

This study shows the results attained during the electrodeposition of Cu_2O films on fluorine-doped tin oxide (FTO) substrate from a dimethyl sulfoxide (DMSO) solution in the presence of chloride ions. Before the film electrodeposition and in order to establish the best conditions for the Cu_2O electrodeposition, a detailed electrochemical study of the precursors in the presence of chloride ions was performed. The voltammetric profiles obtained show significant differences compared to those previously obtained during the study of the Cu_2O electrodeposition from a free-chloride DMSO solution. These differences are the result of the coordination complexes formation between chloride ions and the different copper species in solution. The films were potentiostatically electrodeposited between -1.4 V and -1.6 V vs $\text{Ag}/\text{AgCl}_{(\text{sat})}$ reference electrode. Then, these films were characterized through different techniques: X-ray diffraction, scanning electron microscopy, optical characterization, and capacitance measurements through electrochemical impedance spectroscopy.

Keywords: Cu_2O , Electrodeposition, DMSO solution, Chloride effect.

1. INTRODUCTION

Photovoltaic devices based on metal oxide semiconductors have being a matter of great interest, because to their chemical stability. This way, due to its properties (p-type semiconductor, direct band gap of $2.0 - 2.2$ eV) Cu_2O has been considered an excellent material that can be employed in photovoltaic cells based on p-n junction thin films. Furthermore, Cu_2O is made up of abundant non-toxic elements, which allows it to become a low-cost material¹.

Cu_2O thin films have been prepared through the use of different techniques such as magnetron sputtering²⁻³, chemical vapor deposition⁴⁻⁵, thermal oxidation⁶, and chemical reduction⁷. Electrochemical techniques are easy and inexpensive methods for Cu_2O thin films formation. Copper sulfate in the presence of lactic acid / lactate aqueous solution is usually the most used electrolyte for the electrodeposition of Cu_2O thin film on different substrates⁸⁻¹⁰. However, this research group has recently verified that the electrodeposition of Cu_2O thin films can be carried out from a dimethyl sulfoxide (DMSO) solution, using CuClO_4 and molecular oxygen as precursors¹¹. These films were p-type semiconductors with an optical band gap that varied between 2.18 eV $- 2.25$ eV with a doping level between $8.2 \times 10^{18} \text{ cm}^{-3} - 2.0 \times 10^{19} \text{ cm}^{-3}$, depending on the electrodeposition temperature. On the other hand, it is a well known fact that during the electrodeposition process, the addition of complexing agents produces drastic changes in the morphology and properties of semiconductor materials¹²⁻¹³ and metals¹⁴⁻¹⁵. This way, the influence of chloride ions as a complexing agent during the Cu_2O electrodeposition process from a DMSO solution is analyzed in this article. The results were then compared with those obtained in the absence of chloride ions. The films were smoother than those obtained in the absence of chloride ions, and the doping level was higher, confirming the effect of these anions on the electrodeposited Cu_2O films properties.

2. EXPERIMENTAL SECTION

The electrochemical bath was prepared using CuCl_2 (Aldrich) and LiClO_4 (Merck) and dry dimethyl sulfoxide (DMSO, Merck, max. 0.025% H_2O) as a solvent, without previous treatment. All the electrochemical experiences (voltammetric studies and electrodeposition) were carried out in a potentiostat - galvanostat CH Instrument model CHI-660D connected to the PC. In each case, a conventional three electrodes glass cell that included a working electrode (glassy carbon electrode and fluorine-doped tin oxide (FTO) coated glass slide), a counter electrode (platinum wire) and a reference electrode ($\text{Ag}/\text{AgCl}_{(\text{sat})}$) was employed. All the potentials exhibited in this study are related to this reference electrode. Two substrates were employed as working electrode: a glassy carbon electrode (3 mm diameter, CH Instrument) and a FTO glass slide (TEC 15, XOP Glass, 12-14 W / \square). Before each experience, and in order to clean the electrode surface, the glassy carbon electrode was polished in an aqueous alumina suspension ($0.05 \mu\text{m}$), whereas the FTO substrate was

washed for 10 minutes in acetone and following that for 10 minutes in absolute ethanol inside an ultrasonic cleaner. When the presence of molecular oxygen in the solution was required, a flow of O_2 was bubbled through the solution for 20 minutes, before each experience. During measurements, a stream of O_2 was put over the solution in order to keep an oxygen atmosphere and to assure solution saturation. On the other hand, when no molecular oxygen is required in the solutions, these were bubbled with Ar for 20 minutes. After that, the solutions were put in Ar atmosphere in order to avoid the presence of air in them. A hot plate was used to control the cell temperature through a glycerin bath.

The films of Cu_2O were potentiostatically obtained at different potentials at 80°C on FTO electrodes and were then characterized through different techniques. X-ray diffraction analyses (XRD) were carried out in standard theta - 2 theta scans on a Philips PW180 diffractometer (30kV, 40mA, $\text{CuK}\alpha$ radiation with $\lambda = 1.5406\text{Å}$). The diffraction peaks from Cu_2O have been indexed by reference to the JCPDS powder diffraction files. The morphology of the samples were obtained by scanning electron microscopy (SEM) performed on a SEM LEO 1420 VP, Oxford Instrument, equipped with EDS detector (Energy Dispersive X-ray Spectroscopy). Optical analyses were carried out in a Perkin Elmer spectrophotometer Lambda 35 using a solid sample holder. Measurements of capacitance were carried out between 30 and 10 KHz in a 0.05 M tetraborate buffer solution (pH 9.2) employing an amplitude of 10 mV peak-to-peak.

3. RESULTS AND DISCUSSION

3.1 Voltammetric studies

Figure 1 shows the voltammetric response of a 0.01 M $\text{CuCl}_2 + 0.05$ M LiClO_4 solution on a glassy carbon electrode in the absence of molecular oxygen. In this figure, two cathodic (C1 and C2) and two anodic (A1 and A2) processes can be observed. The cathodic processes are the result of the electrochemical reduction of Cu(II) ions in solution. According to A. Foll et al.¹⁶, Cu^{2+} ion can produce three stable complexes with chloride ions into DMSO solution: CuCl^+ , CuCl_2 and CuCl_3^- . The stability constant of each complex can be observed in Table 1.

Table 1: Cumulative formation constant (β_{ij}) of Cu(II) -chloride and Cu(I) -chloride complexes in DMSO solution, according to Reference (1).

	Cu(II)-Cl complexes			Cu(I)-Cl complexes	
	CuCl^+ β_{11}	CuCl_2 β_{12}	CuCl_3^- β_{13}	CuCl β_{11}	CuCl_2^- β_{12}
Formation Constant (β_{ij})	$10^{4.5}$	$10^{7.5}$	$10^{9.1}$	10^6	$10^{11.95}$

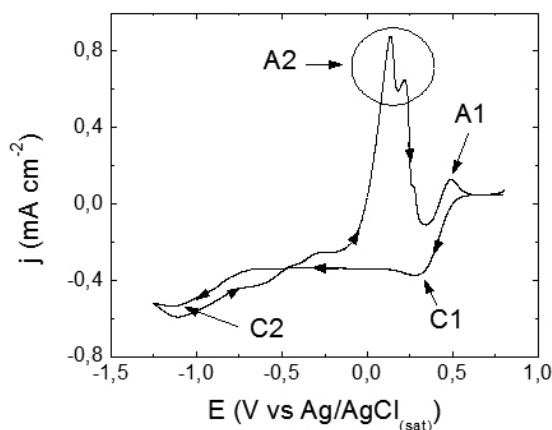


Figure 1: Voltammetric response of a 0.01 M CuCl₂ + 0.05 M LiClO₄ DMSO solution on a glassy carbon electrode in the absence of molecular oxygen at 30° C. Scan rate: 10 mV s⁻¹.

The presence of complexes between Cu(II) and chloride ions has been verified by the color of the solution: when a non-complexing ion is used as an anion (i.e. perchlorate), the color of the solution becomes pale blue (Cu(DMSO)₆²⁺ complex) whereas in this case, the solution is bright yellow (Cu(DMSO)₅Cl₂ complex)¹⁷

On the other hand, Cu⁺ ion can also form two stable complexes when there is chloride ion in a DMSO solution: CuCl and CuCl₂⁻. However, in this study, and according to the distribution diagram (Figure 2) all the existing Cu⁺ is found as CuCl₂⁻ in solution. In the case of Cu(II), the three complexes are found in considerable quantities (Figure 2).

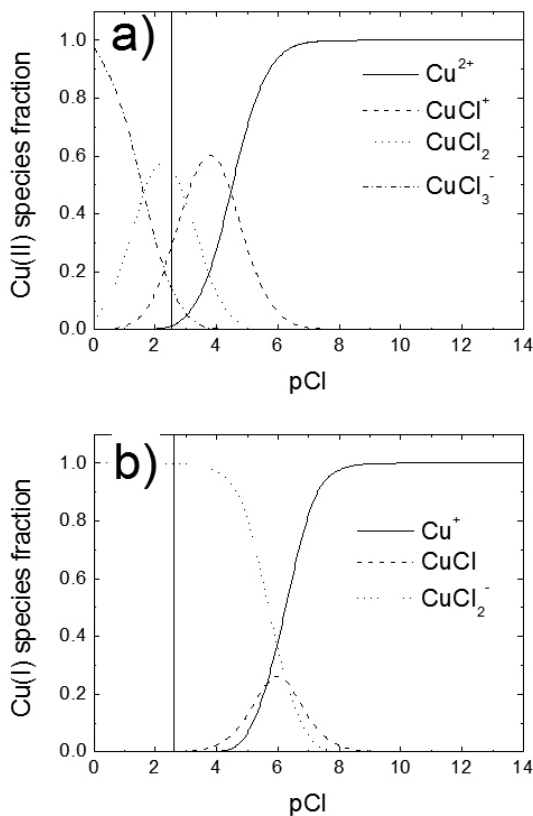


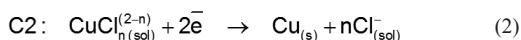
Figure 2: Species distribution diagram for a) Cu(II) and b) Cu(I) complexes in a DMSO solution as a function of pCl according to Table 1. The vertical solid line indicates the free chloride concentration in solution presents in a 0.01 M CuCl₂ DMSO solution.

According to previous studies¹¹, the perchlorate media Cu(II) reduction in a DMSO solution begins by reducing Cu(II) to Cu(I) which exhibits a E_{peak} = 0.050 V vs Ag/AgCl_(sat). This way, in chloride media, the formation of complexes shifts the above potentials to more positive values. Considering the stability constant of both Cu(II) and Cu(I) in chloride media, and the electroneutrality condition of the solution, the shifting of this process should be 250 mV more positive. This shifting process coincides with the E_{peak} observed in Figure 1 (C1 process), where the resulting value is 0.290 V. Therefore, the C1 process has been considered as the reduction of Cu(II) to Cu(I) in chloride media. Thus, according to the latter the following global reaction can be observed:



where n = 1, 2 or 3.

The process assigned as C2 (E_{peak} = -1.150 V) can be inferred as the electrodeposition of copper from Cu(II)-chloride complexes in solution (reaction 2)



In order to confirm the previous reaction, hydrodynamic voltammograms were carried out (Figure 3). In this condition, the process assigned as C2 remains unchanged. The above indicates that the C2 process does not depend on the concentration of species within the electrochemical interphase (Cu(I)), and only depends on the concentration of electrochemically active species in solution (Cu(II)).

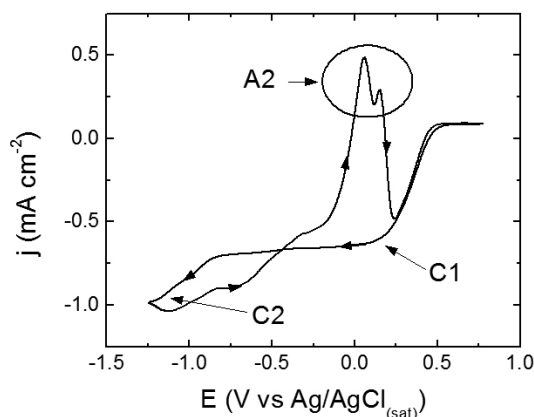
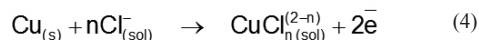
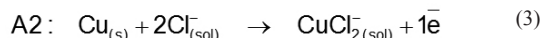
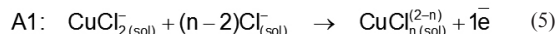


Figure 3: Voltammetric response in hydrodynamic condition (250 rpm) of a 0.01 M CuCl₂ + 0.05 M LiClO₄ DMSO solution on a glassy carbon electrode in absence of molecular oxygen at 30° C. Scan rate: 10 mV s⁻¹.

This way, the anodic process A2 represents the oxidation of elemental copper previously electrodeposited. However, this process shows two components that are not affected by the existing hydrodynamic conditions. According to the standard potentials and stability constants exhibited in Table 1, the most cathodic process is equivalent to the oxidation of elemental copper into Cu(I) and the more anodic process is equivalent to the oxidation of elemental copper into Cu(II), according to the following reactions:



Finally, the process assigned as A1 is a consequence of the oxidation of Cu(I) previously formed in A2 into Cu(II) according to the following reaction:



As CuCl₂⁻ can only be found in the electrochemical interphase, this process is not present when this experience is carried out in hydrodynamic conditions (Figure 3).

When the voltammogram is carried out with molecular oxygen (Figure 4) important changes can be observed. The C1 and A1 processes previously described remain without changes. However, a new cathodic process (C2') at $E_{\text{peak}} = -0.640$ V is observed. Furthermore, the C2 process disappears in the same manner as the anodic processes assigned to A2.

The new cathodic process C2' is the result of the reduction of molecular oxygen in the presence of Cu(II)-chloride and Cu(I)-chloride complexes in solution. Numerous studies^{11, 18-22} have shown that the electroreduction of molecular oxygen in DMSO is a monoelectronic transference followed by different chemical stages. When this process is carried out in presence of a metallic cation, a solid phase corresponding to the metallic oxide is formed. Thus, the C2' process is the consequence of the molecular oxygen reduction which produces copper oxides (Cu_2O and/or CuO). The electrodeposition of these oxides produces a passive electrode surface, diminishing the current as is observed in Figure 4 and avoiding the electrodeposition of elemental copper. As a result of this, the processes assigned to A2 are not found in the voltammogram shown in Figure 4.

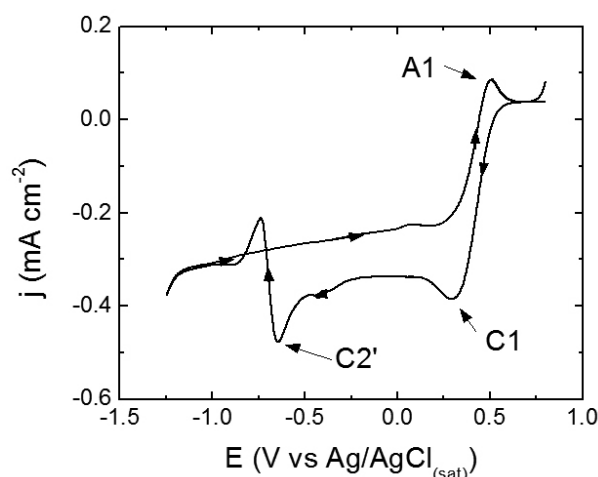


Figure 4: Voltammetric response of a 0.01 M $\text{CuCl}_2 + 0.05$ M LiClO_4 DMSO solution on a glassy carbon electrode in presence of molecular oxygen in solution at 30°C. Scan rate: 10 mV s^{-1} .

When FTO is used as a working electrode, the voltammetric responses are similar to those observed on glassy carbon electrode. Figure 5 shows the voltammogram of a 0.01 M $\text{CuCl}_2 + 0.05$ M LiClO_4 DMSO solution on FTO electrode in presence of molecular oxygen at 30°C. In these conditions, processes C1 and C2' previously described can be clearly observed. The discrepancies in the E_{peak} and in the form of the voltammetric waves are exclusively due to the difference between both substrates employed. In FTO substrate the electroreduction of molecular oxygen begins at -1.00 V and extends to -1.60 V. When the voltammogram is halted at this potential, a yellow-brownish film can be observed on the electrode surface. This film could be the result of Cu_2O film electrodeposition. With potentials that are more negative than -1.60 V, a black film can be observed. Thus, the cathodic process observed between -1.60 V and -2.00 V is the result of the CuO electrodeposition and the substrate reduction. This way, an electrochemical window of 600 mV is established (between -1.0 and -1.6 V) in which the Cu_2O electrodeposition can be performed. This is a potential window wider than that obtained in perchlorate media, in which a narrow window for the Cu_2O electrodeposition is obtained¹¹.

3.2 Film characterization

The electrodeposition of the Cu_2O films on FTO substrate was carried out between the above mentioned potentials, but carried out at 80°C, in order to obtain crystalline films. The best films (homogeneous, yellow-brownish films) were obtained between -1.4 and -1.6 V. In each case, the electrodeposition time was 10 minutes.

Figure 6 shows the XRD pattern of the films obtained at different potentials, together with the Cu_2O JCPDS. As can be observed, the 36.7° and 42.7° film peaks at coincide with the (111) and (200) reflection planes of the Cu_2O diffraction pattern, thus confirming the presence of this compound. No other diffraction peaks, except those of the FTO substrate, can be observed,

proving that no other crystalline compound is found in the films. According to this Figure, it becomes clear that the most crystalline film is that obtained at -1.4 V, which shows sharper peaks than those films obtained at more cathodic potentials. Furthermore, this film shows more intense peaks than those obtained from a DMSO-perchlorate solution¹¹, even at a lower electrodeposition time. Thus, the Cu_2O electrodeposition from DMSO-chloride solutions shows better performance than those that derive from DMSO-perchlorate solutions. The effect of chloride ions on the oxide semiconductor electrodeposition process has been previously studied in both aqueous^{12, 23} and DMSO solutions²². In reference to these studies, it is a well known fact, that chloride ions in aqueous solutions dope ZnO films during their electrodeposition¹². However, these ions do not have an equivalent effect on Cu_2O films when electrodeposited from an alkaline solution²³. In the latter chloride ions modify the morphology of the Cu_2O films and lessen the structural quality as the chloride concentration increases. On the other hand, in a DMSO solution, chloride ions modify both the nucleation and growth mechanisms during the ZnO electrodeposition²². Here, the mechanism varies from instantaneous to progressive growth as a consequence of the complex formation between Zn(II) and chloride ions, and by the adsorption of these ions on the surface of the films. Thus, in the case of Cu_2O , this same effect (complex formation and adsorption on the film surface) would explain the better crystalline character of the films when they are electrodeposited from a chloride bath electrolyte.

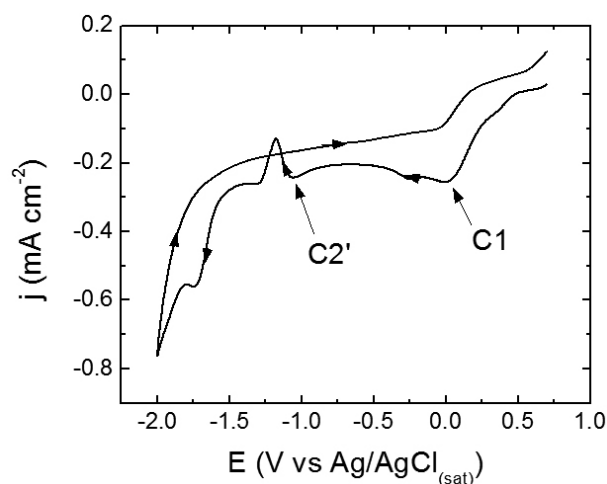


Figure 5: Voltammetric response of a 0.01 M $\text{CuCl}_2 + 0.05$ M LiClO_4 DMSO solution on a FTO electrode in presence of molecular oxygen in solution at 30°C. Scan rate: 10 mV s^{-1} .

Figure 7 shows SEM images of Cu_2O films obtained at -1.4 V and -1.6 V. From these images, it can be observed that the electrodeposited film at -1.4 V is smooth and homogeneous, whereas the film obtained at -1.6 V is globular and rough, which is consistent with the results obtained by XRD. This way, the film formed at -1.4 V has better morphological and structural characteristics than those electrodeposited at more cathodic potentials.

Also, the morphology obtained in both cases, differs from the one obtained from alkaline aqueous solutions, where cubic and pyramidal structures are frequently observed^{9, 23-28}. This kind of morphology has been previously reported for ZnO films electrodeposited from a DMSO solution²⁹. The latter, is a consequence of the anion interaction with the different crystal faces. Therefore, in aqueous solutions, the longitudinal growth of hexagonal ZnO nanowires is favored over the lateral one, due to the reaction of Zn^{2+} with hydroxyl ions adsorbed on the top of the nanowire (polar face (0001)), which hinders the lateral growth³⁰. However, if the chloride ion concentration is increased, these ions will be adsorbed on the top, and will not hinder the lateral growth³¹⁻³². As a result, hexagonal nanowires with different diameters can be performed by controlling the solution composition during the electrodeposition process. In the case of Cu_2O , a similar behavior can be assumed, because of the different adsorption processes reported during its electrosynthesis procedure^{25, 33-34}. When both, ZnO and Cu_2O , are found in a DMSO solution, the absence of hydroxyl ions would prevent the formation of hexagonal and cubic structures, which would result in smooth and homogeneous surfaces.

The optical band gap of the film electrodeposited at -1.4 V was obtained through transmittance measurement (Figure 8).

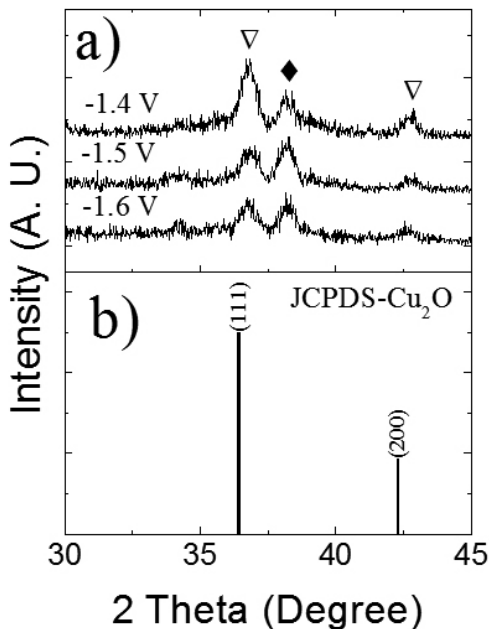


Figure 6: a) XRD pattern of the films obtained between -1.4 and -1.6 V from a 0.01 M CuCl_2 + 0.05 M LiClO_4 DMSO solution on a FTO electrode in presence of molecular oxygen in solution at 80°C . (\blacklozenge) Indicate diffraction peaks which belong to the FTO substrate. (∇) Indicate diffraction peaks belonging to crystalline Cu_2O . b) JCPDS of the Cu_2O .

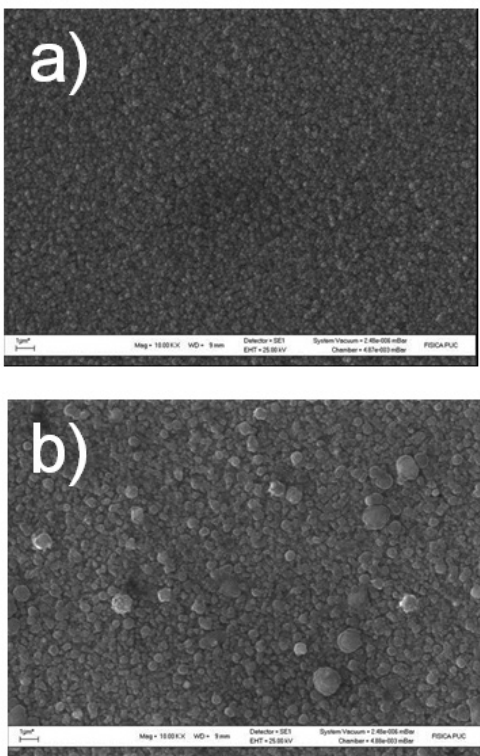


Figure 7: SEM images of Cu_2O films obtained from a 0.01 M CuCl_2 + 0.05 M LiClO_4 DMSO solution on a FTO electrode in the presence of molecular oxygen in solution at 80°C and at different potentials. a) Film electrodeposited at -1.4 V. b) Film electrodeposited at -1.6 V.

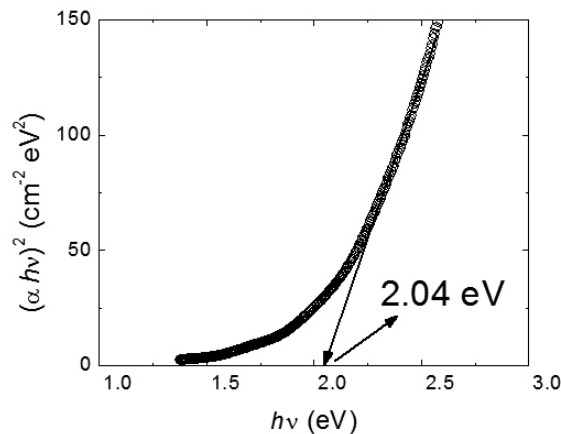


Figure 8: Band gap energy determination for Cu_2O film potentiostatically electrodeposited at -1.4 from a 0.01 M CuCl_2 + 0.05 M LiClO_4 DMSO solution on a FTO electrode in the presence of molecular oxygen at 80°C .

In this case, the absorption coefficient “ α ” is determined through the natural logarithm of the transmittance. When $(\alpha hv)^n$ is plotted against the incident photon energy (hv), a linear relationship is obtained only when $n = 2$, which is consistent with a direct band gap semiconductor³⁵. The above is shown in Figure 8, where an optical band gap (straight line interception with $h\nu$ axis) of 2.04 eV was achieved. This band gap value is somewhat lower than those obtained through electrodeposition from a DMSO solution without chloride ions¹¹.

Finally, capacitance measurements performed through electrochemical impedance spectroscopy techniques, were carried out in order to get the conductivity and doping concentration of the Cu_2O films. These results were shown in a Mott-Schottky plot (Figure 9). In this case, the film electrodeposited at -1.4 V is a p-type semiconductor, which is consistent with what is usually found in related references³⁶. The flat band potential is achieved from the plot intercepts in the potential axis ($C^{-2} = 0$). As can be observed, the flat band potentials are almost independent of the frequency, varying between 0.950 V (10 KHz) to 1.04 V (30 KHz). However, the slopes vary according to the frequency, which result in doping levels that range from $1.9 \times 10^{19} \text{ cm}^{-3}$ at 30 KHz to $1.5 \times 10^{20} \text{ cm}^{-3}$ at 10 KHz. Although in theory it is widely assumed that the slope in the Mott-Schottky plots should be frequency independent, the effects of surface roughness, dielectric relaxation together with the presence of surface states, can originate a frequency dispersion in the slope, and which is frequently found in these kind of measurements³⁷. On the other hand, the above mentioned doping levels are higher than the accepted values for typical semiconductors ($\sim 10^{18} \text{ cm}^{-3}$) due to the chloride incorporated in the film. This produces a high concentration of surface-states, which in turn provoke a high acceptor concentration. The arguments above are consistent with the variation of doping levels related to the frequency, as previously discussed.

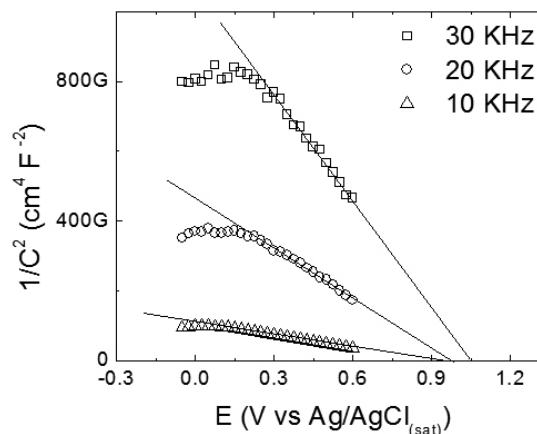


Figure 9: Mott-Schottky plot, at different frequencies, of a Cu_2O film obtained at -1.4 V from a 0.01 M CuCl_2 + 0.05 M LiClO_4 DMSO solution on a FTO electrode in the presence of molecular oxygen at 80°C .

4. CONCLUSION

The Cu₂O electrodeposition from a DMSO solution in the presence of chloride ions was studied using CuCl₂ and molecular oxygen as precursors. Under these conditions, p-type Cu₂O films can be electrodeposited on FTO substrate between -1.4 and -1.6 V. As opposed to the electrodeposition in the absence of chloride (perchlorate media), a wider electrochemical window with more cathodic potential values was obtained. The above is explained by the formation of different complexes between Cu²⁺ and Cu⁺ with chloride ions, displacing the electroactive zone where the Cu₂O can be electrodeposited. The presence of chloride ions improves the film crystalline character when compared with the films electrodeposited in the absence of this anion. Smooth and homogeneous films were obtained at -1.4 V, with an optical band gap value of 2.04 eV. A high doping level (10¹⁹ to 10²⁰ cm⁻³) was determined through Mott-Schottky plots. The above is a consequence of surface states, which are produced by the presence of chloride ions during the electrodeposition process.

ACKNOWLEDGEMENTS

This study was financed by FONDECYT (Chile) project 1110546.

M. León appreciates the support given by CONICYT-PCHA / Doctorado Nacional / Año 2015-Folio 21150057, and PIIC-2015 DGIP-UTFSM

REFERENCES

- S. Rühle, A. Y. Anderson, H.-N. Barad, B. Kupfer, Y. Bouhadana, E. Rosh-Hodesh and A. Zaban, *J. Phys. Chem. Lett.*, **3**, 3755, (2012).
- C. Liu, Z. D. Wei, Q. Zhang, B. S. Hu, X. Q. Qi, S. G. Chen and W. Ding, *J. Inorg. Mater.*, **27**, 395, (2012).
- B. B. Li, L. Lin, H. L. Shen, F. E. Boafu, Z. F. Chen, B. Liu and R. Zhang, *Eur. Phys J-Appl. Phys.*, **58**, 20303, (2012).
- A. El Kasmi, Z. Y. Tian, H. Vieker, A. Beyer and T. Chafik, *Appl. Catal., B*, **186**, 10, (2016).
- S. Eisermann, A. Kronenberger, A. Laufer, J. Bieber, G. Haas, S. Lautenschlager, G. Homm, P. J. Klar and B. K. Meyer, *Phys. Status Solidi A*, **209**, 531, (2012).
- S. Mani, J. I. Jang, J. B. Ketterson and H. Y. Park, *J. Cryst. Growth*, **311**, 3549, (2009).
- D. Dodoo-Arhin, M. Leoni, P. Scardi, E. Garnier and A. Mittiga, *Mater. Chem. Phys.*, **122**, 602, (2010).
- T. Mahalingam, J. S. P. Chitra, J. P. Chu, S. Velumani and P. J. Sebastian, *Sol. Energy Mater. Sol. Cells*, **88**, 209, (2005).
- W. Septina, S. Ikeda, M. A. Khan, T. Hirai, T. Harada, M. Matsumura and L. M. Peter, *Electrochim. Acta*, **56**, 4882, (2011).
- V. Georgieva and M. Ristov, *Sol. Energy Mater. Sol. Cells*, **73**, 67, (2002).
- G. Riveros, A. Garmendia, D. Ramirez, M. Tejos, P. Grez, H. Gomez and E. A. Dalchiele, *J. Electrochem. Soc.*, **160**, D28, (2013).
- J. Rousset, E. Saucedo and D. Lincot, *Chem. Mater.*, **21**, 534, (2009).
- P. H. Quang, T. B. H. Dang, N. D. Sang, T. H. Duc and L. T. Tu, *J. Ceram. Process. Res.*, **13**, S318, (2012).
- G. Y. Wei, J. W. Lou, H. L. Ge, Y. D. Yu, L. Jiang and L. X. Sun, *Surf. Eng.*, **28**, 412, (2012).
- L. C. Melo, P. de Lima-Neto and A. N. Correia, *J. Appl. Electrochem.*, **41**, 415, (2011).
- A. Foll, M. Le Démezet and J. Courtot-Coupez, *J. Electroanal. Chem. Interfacial Electrochem.*, **35**, 41, (1972).
- A. G. Massey, B. F. G. Johnson, N. R. Thompson and R. Davis, *The Chemistry of Copper, Silver and Gold*, Pergamon Press, Oxford, 1973.
- H. Gomez, G. Riveros, D. Ramirez, R. Henriquez, R. Schrebler, R. Marotti and E. Dalchiele, *J. Solid State Electrochem.*, **16**, 197, (2012).
- R. Henriquez, M. Froment, G. Riveros, E. A. Dalchiele, H. Gomez, P. Grez and D. Lincot, *J. Phys. Chem. C*, **111**, 6017, (2007).
- R. Henriquez, H. Gomez, P. Grez, D. Lincot, M. Froment, E. A. Dalchiele and G. Riveros, *Electrochem. Solid-State Lett.*, **10**, D134, (2007).
- M. E. Ortiz, L. J. Nunez-Vergara and J. A. Squella, *J. Electroanal. Chem.*, **519**, 46, (2002).
- G. Riveros, D. Ramirez, A. Tello, R. Schrebler, R. Henriquez and H. Gomez, *J. Brazil. Chem. Soc.*, **23**, 505, (2012).
- S. Haller, J. Jung, J. Rousset and D. Lincot, *Electrochim. Acta*, **82**, 402, (2012).
- F. Sun, Y. P. Guo, Y. M. Tian, J. D. Zhang, X. T. Lv, M. G. Li, Y. H. Zheng and Z. C. Wang, *J. Cryst. Growth*, **310**, 318, (2008).
- M. J. Siegfried and K. S. Choi, *Adv. Mater.*, **16**, 1743, (2004).
- T. D. Golden, M. G. Shumsky, Y. C. Zhou, R. A. VanderWerf, R. A. VanLeeuwen and J. A. Switzer, *Chem. Mater.*, **8**, 2499, (1996).
- Y. C. Zhai, H. Q. Fan, Q. Li and W. Yan, *Appl. Surf. Sci.*, **258**, 3232, (2012).
- A. Paracchino, J. C. Brauer, J. E. Moser, E. Thimsen and M. Graetzel, *J. Phys. Chem. C*, **116**, 7341, (2012).
- A. Tello, H. Gomez, E. Munoz, G. Riveros, C. J. Pereyra, E. A. Dalchiele and R. E. Marotti, *J. Electrochem. Soc.*, **159**, D750, (2012).
- J. Elias, R. Tena-Zaera and C. Levy-Clement, *J. Electroanal. Chem.*, **621**, 171, (2008).
- R. Tena-Zaera, J. Elias, G. Wang and C. Levy-Clement, *J. Phys. Chem. C*, **111**, 16706, (2007).
- S. Sanchez, C. Levy-Clement and V. Ivanova, *J. Electrochem. Soc.*, **159**, D705, (2012).
- J. H. Zhong, G. R. Li, Z. L. Wang, Y. N. Ou and Y. X. Tong, *Inorg. Chem.*, **50**, 757, (2011).
- S. Yoon, S. D. Kim, S. Y. Choi, J. H. Lim and B. Yoo, *Cryst. Growth Des.*, **15**, 4969, (2015).
- M. Sreemany and S. Sen, *Mater. Chem. Phys.*, **83**, 169, (2004).
- Y. Nakano, S. Saeki and T. Morikawa, *Appl. Phys. Lett.*, **94**, 022111, (2009).
- W. P. Gomes and F. Cardon, *Prog. Surf. Sci.*, **12**, 155, (1982).